Simultaneous Measurement of Magnetic Vortex Polarity and Chirality using Scanning Electron Microscopy with Polarization Analysis (SEMPA)

S.-H. Chung[1,2], D. T. Pierce[1], and J. Unguris[1]

[1]*Center for Nanoscale Science and Technology, National Institute of Standards and Technology, Gaithersburg, MD 20899*

[2]*Maryland NanoCenter, University of Maryland, College Park, MD, 20742*

(June 25, 2009)

The magnetic vortex structure is an equilibrium configuration frequently found in patterned magnetic nanostructures. It is characterized by an in-plane curling of the magnetization with clockwise or anticlockwise chirality and by an out of plane vortex core that can have a positive or negative polarity. The small size of the vortex core, on the order of 10 nm, makes it technologically interesting, but also difficult to measure or image directly. In this work, we used Scanning Electron Microscopy with Polarization Analysis (SEMPA) to directly image magnetic vortex cores in patterned NiFe/Ta bilayer structures. With SEMPA we can simultaneously measure the in-plane and the out-of-plane component of the surface magnetization and thereby determine both the vortex chirality and the vortex core polarity in a single measurement. Our magnetic simulation of the vortex core, considering only the exchange and magnetostatic energy, is in good agreement with the SEMPA measurement of the magnetization when other experimental factors are taken into account.

1. **Introduction**

    The magnetic vortex state is an equilibrium configuration found, for example, in submicron magnetic disks with diameters and thicknesses within a certain range.[1] The vortex state in magnetic nanostructures has excited considerable interest because of its potential application in magnetic memory and storage. In the vortex state, the magnetization forms a flux-closed loop following the circumference of the disk, the sense of which is its chirality. The magnetization turns toward the surface normal in the vortex core, either into or out of the plane which determines its polarity. The polarity determines the sense of the vortex core gyration in the in-plane excitation mode.[2] The vortex state has been investigated for potential data storage applications by switching the vortex core polarity.[3,4] Both the static and dynamic properties of the magnetic vortex are strongly influenced by the chirality and the polarity. Because of both scientific and technological interest, considerable effort has been put toward measuring the properties of the vortex state. What has been elusive to date has been a direct determination of the chirality and polarity of the vortex in the same measurement. In this work, we show that Scanning Electron Microscopy with Polarization Analysis (SEMPA) can directly image the magnetic vortex and simultaneously determine both the vortex polarity and chirality.

    The measurement of both the chirality and the polarity of the magnetic vortex presents a challenge for magnetic imaging techniques that is compounded by the small

size of the vortex core. For example, the vortex core is too small to be resolved by conventional magneto-optic imaging. Magnetic force microscopy (MFM) can detect the vortex core with good sensitivity to the out-of-plane stray field[5], but with the poor in-plane sensitivity and lateral resolution. MFM can only provide vortex polarity information. Spin polarized scanning tunneling microscopy (SP-STM) can image both in-plane and out-of-plane magnetization with atomic resolution[6]. However, SP-STM cannot determine the vortex chirality and polarity at the same time since it requires different scanning tip conditions for the in-plane and out-of-plane measurement. SP-STM also requires a single crystal film with well defined band structure. Magnetic x-ray microscopy[2,3] can only measure the component of magnetization along the photon propagation direction. Transmission electron microscopy (TEM) methods, such as electron holography or Lorentz TEM[7], typically do not determine the chirality and polarity in a single measurement. However, very recently, Phatak *et al.*[8] showed how the polarity and chirality could be determined from a single Lorentz Fresnel image, and suggest that with further microscope improvements quantitative measurements may be possible. In this paper, we present SEMPA results demonstrating quantitative measurements of the magnetic vortex magnetization including the chirality and the polarity.

2. Simulation

The features of the magnetic vortex configuration are illustrated by the micromagnetic simulation shown in Fig. 1, which we performed using the public domain OOMMF code[9]. The simulation is for a NiFe disk with diameter, $D = 200$ nm, and thickness, $T = 20$ nm. The material parameters used for NiFe were the saturation

magnetization $M_s = 8.0 \times 10^5$ A/m and the exchange stiffness $A = 1.3 \times 10^{-11}$ J/m. The crystalline anisotropy was neglected. The unit cell size for this 2-D simulation was 1×1 nm^2. The minimum energy state was approached from the initial randomly magnetized state. Figure 1 shows both (a) in-plane and (b) out-of-plane components of the surface magnetization of the NiFe disk. The in-plane magnetization in the ground state exhibits curling around the center of the disk to reduce magnetostatic energy. The chirality of the curling can be clockwise or counter-clockwise. Near the center of the disk the magnetization turns into the out-of-plane direction to compensate the extremely large exchange energy due to the antiparallel arrangement of in-plane spins. This vortex core region is clearly shown in Fig. 2(b). The magnetization along the surface normal can be out of the plane with positive polarity, or into the plane with negative polarity. Fig. 2(c) shows a cut through the vortex core. The points are from the simulation and the line is a Gaussian fit with a FWHM of 18.3 nm. Interestingly, the simulation shows a weak magnetization opposite to the vortex core at its base; this has been discussed previously[1] and observed in spin polarized scanning tunneling spectroscopy experiments.[6] However, the Gaussian is a good first order fit to the simulation and will be used below in analyzing the SEMPA data. The analytical theory predicts that the core size is determined mainly by two material parameters, the exchange stiffness and saturation magnetization,[10] and is also independent of the lateral shape and the disk diameter in the vortex forming regime.[11]

3. Experiment

The principle of SEMPA is based on the fact that the spin orientation of the secondary electrons emitted from the surface of a ferromagnetic material is antiparallel to

the magnetization at the point of origin.[12,13] As the unpolarized incident electron beam

from an SEM is rastered on the sample surface, the topographic image from the

secondary electron intensity and the magnetization image from the difference between

the numbers of spin-up and spin-down electrons, i.e. the spin polarization,

$P = (N_\uparrow - N_\downarrow)/(N_\uparrow + N_\downarrow)$, are recorded simultaneously by a spin-polarization analyzer.

Our spin analyzers measure two components of M simultaneously: either M_x and M_y or

M_x and M_z. Fig. 2 shows the intensity and in-plane magnetization images of NiFe disks

measured simultaneously. The samples consisted of NiFe (25nm) / Ta (3nm), on 80 nm

of SiN on a Si substrate, patterned by electron beam lithography and lift-off into disks

with various diameters. The topography image from the intensity measurement is shown

in Fig. 2(a), and the two components of the magnetization, M_x and M_y, are shown in Fig

2 (b) and (c). The in-plane magnetization angle, $\tan^{-1}(M_y / M_x)$, was constructed from

the two in-plane magnetization images (b) and (c) and plotted in Fig. 2(d), which clearly

shows the different vortex chirality of each disk with the magnetization directions

represented by a color wheel. Note, however, that the chirality can be determined from

only either the M_x or M_y image. The topography of the zoomed-in image in Fig. 2(e)

shows ~10 nm size grain features on the surface of NiFe film. The corresponding in-

plane magnetization image in Fig. 2(f) has counter-clockwise vortex chirality. The circled

region in Fig. 2(e) corresponding to the vortex center does not have any distinctive

topographical features. However, in some cases, we found that the topographical features

such as small defects near the center of disks behave as pinning centers of the vortex

cores. SEMPA is operated under ultrahigh vacuum since magnetic contrast is sensitive to

surface contamination. Sample surfaces are often coated with a few atomic layers of Fe to

enhance magnetic contrast and also to prevent charging in non-conductive magnetic samples. We have not observed any change in the magnetic structure due to this very thin Fe layer. In this work, the SEMPA imaging was performed at room temperature.

Additionally, by bending the beam of secondary electrons by 90 degrees into a second spin-polarization analyzer, SEMPA can provide one in-plane and one out-of-plane magnetization image simultaneously. Figure 3 shows the simultaneous measurement of the intensity, the in-plane magnetization component M_x and the out-of-plane magnetization component M_z near the center of two different 1 μm diameter disks. A median filter has been applied to the images to remove some noise, and the images have been processed to compensate for a slight misalignment between the sample surface and the spin analyzer axes. The M_x images in Fig. 3(a) and Fig. 3(b) show that both disks have the same counter-clockwise chirality. The M_z images show a bright magnetic contrast at the center of the vortex in Fig. 3(a) and a dark magnetic contrast in Fig. 3(b). This means that the two disks have the same vortex chirality but the opposite core polarity. This observation demonstrates that high-resolution SEMPA can indeed measure both vortex chirality and polarity simultaneously in single measurement. Identifying the vortex core location, marked by the circles, is greatly helped by using the high contrast M_x image to find the center of the vortex.

4. Analysis and discussion

To obtain quantitative information about the M_x and M_z magnetization in the vortex structure, we show in Fig. 4 (a) the values of the polarization along the dashed line in the M_x image of Fig. 3(a). The polarization changes from -0.17 to +0.17 on going through the vortex core. The polarization arising from the M_z magnetization of the vortex core is

rather small and the signal is noisy. We show in Fig. 4 (b) the values of the polarization along the dashed line in the M_z image in Fig. 3 (a). The noise corresponds to a polarization of P=±0.007. To take advantage of all of the data, we fit a symmetric two-dimensional Gaussian of the following form to the vortex core image:

$$M_z = A_0 + A_1 \exp[-\frac{1}{2}(\frac{x-x_0}{\sigma})^2 - \frac{1}{2}(\frac{y-y_0}{\sigma})^2].$$

For example, in the case of the positive polarity peak in Fig. 3(a), the offset A_0 is negligible, the peak height A_1 is 0.026, and $\sigma = 12.5 \pm 0.5$ nm where the 0.5 nm uncertainty represents one standard deviation in the fit. Similarly, for the negative polarity peak, A_1 is 0.014, and $\sigma = 10.4 \pm 0.8$ nm.

We normalized the z-component of the magnetization from Fig. 3(a) and 3(b) to the x-component of the magnetization away from the vortex core. The value of M_x away from the vortex core in a region where only the x-component of magnetization is present is a good approximation of *M*. In Fig. 4(c) we display the $|M_z / M|$ profiles for both the positive polarity (green) and negative polarity (red) vortex cores obtained from the two-dimensional Gaussian function fits to the data. The full width half maximum of the positive and negative vortex cores are 29.4 and 24.5 nm respectively. This result shows that SEMPA can resolve the magnetic vortex core with sufficient signal to noise to obtain quantitative information by counting the spin-polarized electrons that originate from a very small region of the sample surface (~1 nm of probing depth).

Also shown in Fig. 4(c) is the vortex core profile, $|M_z / M|$, from the OOMF simulation of Fig. 1. In comparing the simulated and measured profiles, we have to consider instrumental and other contributions to the measurement. There are two main

contributions to the secondary electrons measured in the spin analyzers. First there are the

Type I secondaries generated within the incident SEM beam diameter. The diameter of

the incident beam contributes to the apparent diameter of a measured feature. Moreover,

if the incident beam is larger than the feature to be measured, secondaries from

neighboring regions are added to the signal. In the case of the vortex core, secondary

electrons generated outside the vortex core reduce the overall magnitude of the

polarization from the vortex core. Thus, the incident beam broadens and reduces the

magnitude of the measured vortex core. A 20 nm FWHM SEM beam profile convolved

with the simulated vortex core gives a profile of 27 nm FWHM and 0.44 of the initial

height.

Additionally there are Type II secondary electrons generated by backscattered

electrons over an area of order one micrometer diameter. (Note that Type III secondary

electrons are not collected by the SEMPA input optics.) Because of the broadness of the

Type II distribution, all parts of the vortex core image are affected in the same way.

Hence, the Type II secondary electrons decrease the magnitude of M_z in the image of the

vortex core but do not change the apparent core diameter. If 50% of the secondaries are

Type II secondaries, the height of the vortex core would be reduced from 0.44 to 0.22,

approaching the experimentally measured value. A detailed discussion of the role of Type

II secondaries in SEMPA will be presented elsewhere.

Finally, we should note that although the measured vortices and OOMMF

simulation seem to agree, there is uncertainty in the simulation. Specifically, the granular,

polycrystalline film structure seen in the SEMPA topography images is not the same as

the ideal, perfect films modeled in the OOMMF simulation. Understanding how the

vortices interact with the real film structure is an important question about vortex behavior in nanomagnetic structures.

5. Conclusion

In conclusion, from SEMPA images of a NiFe/Ta bilayer, we have demonstrated that SEMPA can determine both the vortex chirality and the vortex polarity with a single measurement. The comparison of the micromagnetic simulation based on exchange and magnetostatic energy showed reasonable agreement with the experimental data after taking into account contributions from the instrument and from Type II secondary electrons.

Figure Captions

FIG. 1. Micromagnetic simulation of the magnetic ground state of a NiFe nanodisk (200 nm in diameter and 20 nm in thickness). (a) is the in-plane component and (b) is the out-of-plane component of the surface magnetization. (c) shows a profile of the simulation (points) along the line in (b). The full line is a Gaussian fit to the simulation profile.

FIG. 2. SEMPA images of the 25 nm thick NiFe disks. (a) intensity displaying the topography, (b) x-component of magnetization, (c) y-component of magnetization, (d) angle of magnetization represented by the color wheel, (e) zoomed-in view of the topography near the center of a disk, and (f) the zoomed-in view of the angle map of the in-plane magnetization.

FIG. 3. SEMPA images near the center of two 25 nm thick NiFe disks. (a) and (b) show from left to right, intensity, the corresponding M_x component, the corresponding M_z component measured simultaneously. The images in (a) and (b) show that the two magnetic vortices have the same chirality but the opposite polarity.

FIG. 4. (a) A line scan through the M_x image in Fig. 3 (a) shows the change in the polarization in the x direction on going through the vortex. (b) A line scan through the M_z image in Fig. 3(a) shows the variation in the z-component of polarization at the vortex. (c) A comparison of the $|M_z/M|$ profile from the simulated vortex core and the

normalized $|M_z / M|$ profiles from the two-dimensional Gaussian fit to images displaying
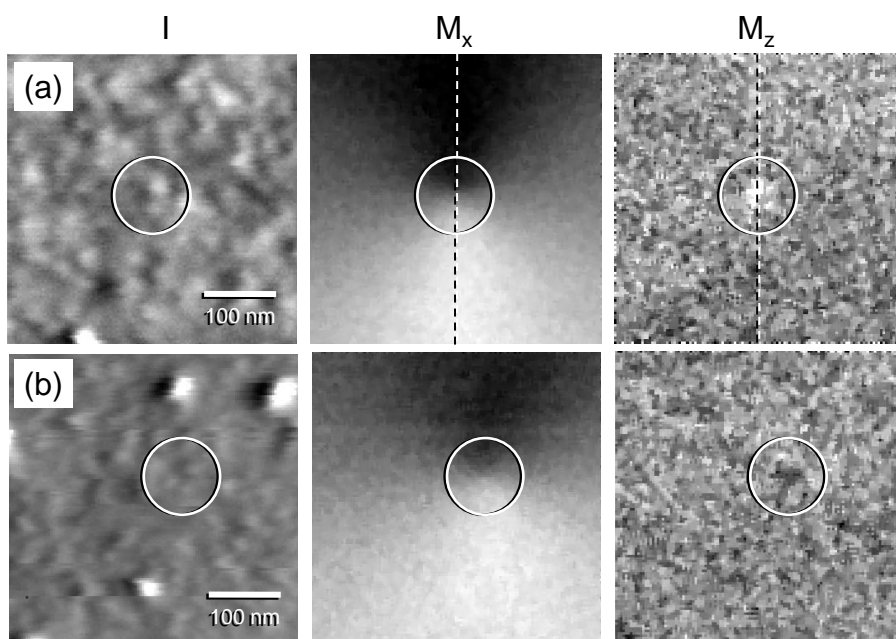
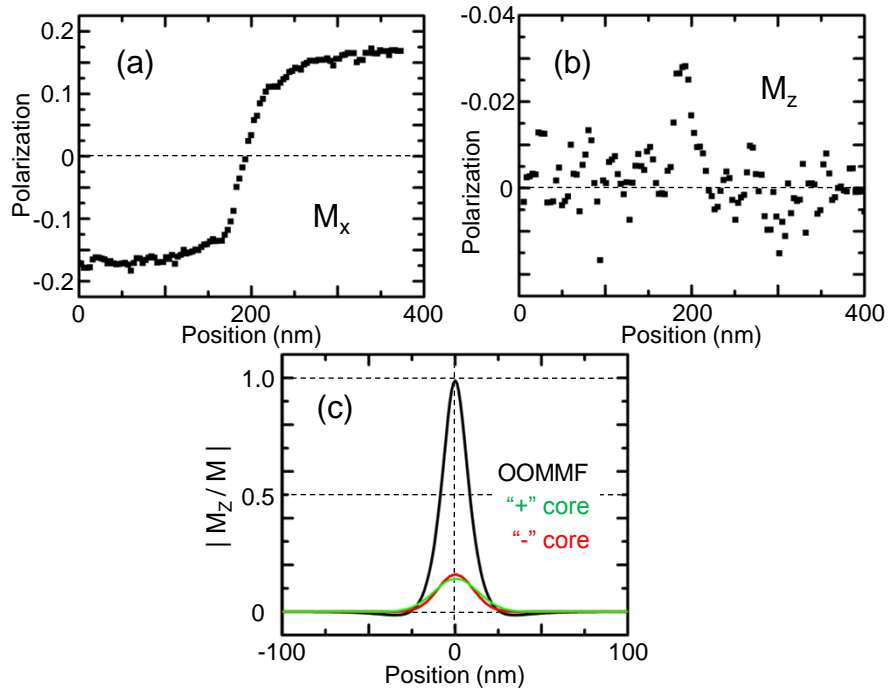positive and negative polarity vortex cores.

FIG. 1
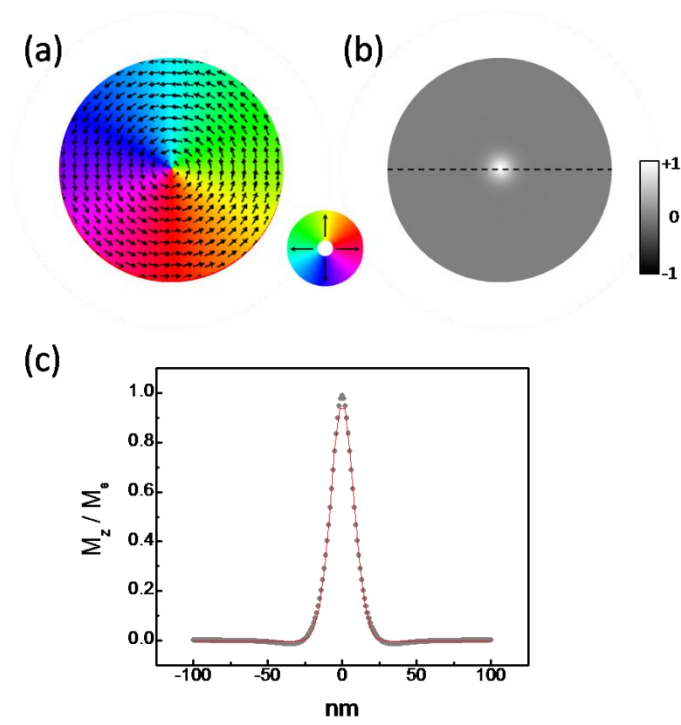
FIG. 2
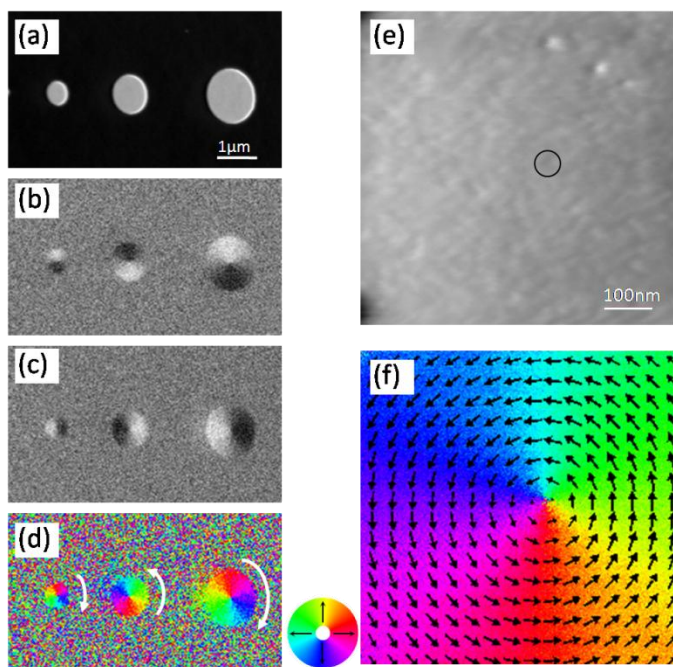
FIG. 3

FIG. 4

References

[1] A. Hubert and R. Schafer, Magnetic Domains – the Analysis of Magnetic Microstructures, Springer, Berlin (1998).

[2] S.-B. Choe, Y. Acremann, A. Scholl, A. Bauer, A. Doran, J. Stohr, and H. A. Padmore, Science **304**, 420 (2004).

[3] B. Van Waeyenberge *et al*. Nature **444**, 461 (2006).

[4] K. Yamada, S. Kasai, Y. Nakatani, K. Kobayashi, H. Kohno, A. Thiaville, and T. Ono, Nature Materials **6**, 270 (2007).

[5] T. Shinjo, T. Okuno, R. Hassdorf, K. Shigeto, and T. Ono, Science **289**, 930 (2000).

[6] A. Wachowiak, J. Wiebe, M. Bode, O. Pietzsch, M. Morgenstern, and R. Wiesendanger, Science **298**, 577 (2002).

[7] M. De Graef, and Y. Zhu (Eds.), Magnetic Microscopy and its Applications to Magnetic Materials, Experimental Methods in the Physical Sciences, Vol 36, Academic Press, New York, 2000.

[8] C. Phatak, M. Tanase, A.K. Petford-Long, and M. De Graef, Ultramicroscopy **109**, 264 (2009).

[9] http://math.nist.gov/oommf/bibiography.html.

[10] E. Feldtkeller and H. Thomas, Phys. Kondens. Mater. **4**, 8 (1965).

[11] C. A. Ross *et al*., Phy. Rev. B **65**, 144417 (2002).

[12] M. R. Scheinfein, J. Unguris, M. H. Kelley, D. T. Pierce, and R. J. Celotta, Rev. Sci. Instrum. **61**, 2501 (1990).

[13] J. Unguris, "SEMPA and its Applications," in *Experimental Methods in the Physical Sciences* **36**, eds. M. De Graef and Y. Zhu, Academic Press, New York (2001) p. 167-194.